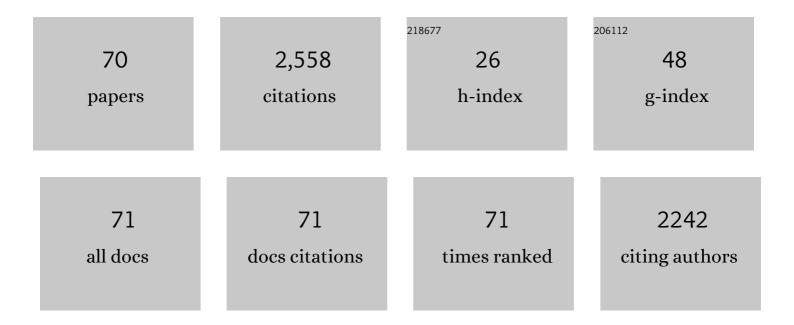
Yuka Otaki

List of Publications by Year in descending order

Source: https://exaly.com/author-pdf/11200378/publications.pdf Version: 2024-02-01



#	Article	IF	CITATIONS
1	Automated quantitative analysis of CZT SPECT stratifies cardiovascular risk in the obese population: Analysis of the REFINE SPECT registry. Journal of Nuclear Cardiology, 2022, 29, 727-736.	2.1	11
2	Value of semiquantitative assessment of high-risk plaque features on coronary CT angiography over stenosis in selection of studies for FFRct. Journal of Cardiovascular Computed Tomography, 2022, 16, 27-33.	1.3	8
3	Diagnostic safety of a machine learning-based automatic patient selection algorithm for stress-only myocardial perfusion SPECT. Journal of Nuclear Cardiology, 2022, 29, 2295-2307.	2.1	21
4	Clinical Deployment of Explainable Artificial Intelligence of SPECT for Diagnosis of Coronary Artery Disease. JACC: Cardiovascular Imaging, 2022, 15, 1091-1102.	5.3	44
5	Determining a minimum set of variables for machine learning cardiovascular event prediction: results from REFINE SPECT registry. Cardiovascular Research, 2022, 118, 2152-2164.	3.8	26
6	Prognostic value of early left ventricular ejection fraction reserve during regadenoson stress solid-state SPECT-MPI. Journal of Nuclear Cardiology, 2022, 29, 1219-1230.	2.1	5
7	The application of artificial intelligence in nuclear cardiology. Annals of Nuclear Medicine, 2022, 36, 111-122.	2.2	9
8	Deep learning-enabled coronary CT angiography for plaque and stenosis quantification and cardiac risk prediction: an international multicentre study. The Lancet Digital Health, 2022, 4, e256-e265.	12.3	85
9	Calcium scoring in low-dose ungated chest CT scans using convolutional long-short term memory networks. , 2022, , .		2
10	Improved myocardial blood flow estimation with residual activity correction and motion correction in 18F-flurpiridaz PET myocardial perfusion imaging. European Journal of Nuclear Medicine and Molecular Imaging, 2022, 49, 1881-1893.	6.4	9
11	Relationship between ischaemia, coronary artery calcium scores, and major adverse cardiovascular events. European Heart Journal Cardiovascular Imaging, 2022, 23, 1423-1433.	1.2	16
12	Explainable Deep Learning Improves Physician Interpretation of Myocardial Perfusion Imaging. Journal of Nuclear Medicine, 2022, , jnumed.121.263686.	5.0	7
13	Differences in Prognostic Value of Myocardial Perfusion Single-Photon Emission Computed Tomography Using High-Efficiency Solid-State Detector Between Men and Women in a Large International Multicenter Study. Circulation: Cardiovascular Imaging, 2022, 15, .	2.6	2
14	Quantification of myocardial blood flow by CZT-SPECT with motion correction and comparison with 15O-water PET. Journal of Nuclear Cardiology, 2021, 28, 1477-1486.	2.1	31
15	Short-term repeatability of myocardial blood flow using 82Rb PET/CT: The effect of arterial input function position and motion correction. Journal of Nuclear Cardiology, 2021, 28, 1718-1725.	2.1	20
16	Elucidating the pathophysiology of left bundle branch block related perfusion defects. Journal of Nuclear Cardiology, 2021, 28, 2923-2926.	2.1	1
17	Prediction of revascularization by coronary CT angiography using a machine learning ischemia risk score. European Radiology, 2021, 31, 1227-1235.	4.5	15
18	Quantitation of Poststress Change in Ventricular Morphology Improves Risk Stratification. Journal of Nuclear Medicine, 2021, 62, 1582-1590.	5.0	7

Υυκά Οτακι

#	Article	IF	CITATIONS
19	Impact of Early Revascularization on Major Adverse Cardiovascular Events inÂRelation to Automatically QuantifiedÂlschemia. JACC: Cardiovascular Imaging, 2021, 14, 644-653.	5.3	28
20	Clinical Utility of SPECT in the Heart Transplant Population. Transplantation, 2021, Publish Ahead of Print, .	1.0	4
21	Prognostic Value of Phase Analysis for Predicting Adverse Cardiac Events Beyond Conventional Single-Photon Emission Computed Tomography Variables: Results From the REFINE SPECT Registry. Circulation: Cardiovascular Imaging, 2021, 14, e012386.	2.6	13
22	Diagnostic Accuracy of CardiovascularÂMagnetic Resonance for Cardiac Transplant Rejection. JACC: Cardiovascular Imaging, 2021, 14, 2337-2349.	5.3	10
23	The accuracy of coronary CT angiography in patients with coronary calcium score above 1000 Agatston Units: Comparison with quantitative coronary angiography. Journal of Cardiovascular Computed Tomography, 2021, 15, 412-418.	1.3	13
24	Simulation of Low-Dose Protocols for Myocardial Perfusion ⁸² Rb Imaging. Journal of Nuclear Medicine, 2021, 62, 1112-1117.	5.0	6
25	Computed tomography angiography-derived extracellular volume fraction predicts early recovery of left ventricular systolic function after transcatheter aortic valve replacement. European Heart Journal Cardiovascular Imaging, 2021, 22, 179-185.	1.2	20
26	Upper reference limits of transient ischemic dilation ratio for different protocols on new-generation cadmium zinc telluride cameras: A report from REFINE SPECT registry. Journal of Nuclear Cardiology, 2020, 27, 1180-1189.	2.1	17
27	Predictors of 18F-sodium fluoride uptake in patients with stable coronary artery disease and adverse plaque features on computed tomography angiography. European Heart Journal Cardiovascular Imaging, 2020, 21, 58-66.	1.2	50
28	Simultaneous Tc-99m PYP/TI-201 dual-isotope SPECT myocardial imaging in patients with suspected cardiac amyloidosis. Journal of Nuclear Cardiology, 2020, 27, 28-37.	2.1	25
29	Optimization of reconstruction and quantification of motion-corrected coronary PET-CT. Journal of Nuclear Cardiology, 2020, 27, 494-504.	2.1	43
30	Rationale and design of the REgistry of Fast Myocardial Perfusion Imaging with NExt generation SPECT (REFINE SPECT). Journal of Nuclear Cardiology, 2020, 27, 1010-1021.	2.1	74
31	5-Year Prognostic Value of QuantitativeÂVersus Visual MPI in SubtleÂPerfusionÂDefects. JACC: Cardiovascular Imaging, 2020, 13, 774-785.	5.3	70
32	Machine learning predicts per-vessel early coronary revascularization after fast myocardial perfusion SPECT: results from multicentre REFINE SPECT registry. European Heart Journal Cardiovascular Imaging, 2020, 21, 549-559.	1.2	70
33	The association between epicardial adipose tissue thickness around the right ventricular free wall evaluated by transthoracic echocardiography and left atrial appendage function. International Journal of Cardiovascular Imaging, 2020, 36, 585-593.	1.5	2
34	The Impact of Valvuloarterial Impedance on Left Ventricular Geometrical Change after Transcatheter Aortic Valve Replacement: A Comparison between Valvuloarterial Impedance and Mean Pressure Gradient. Journal of Clinical Medicine, 2020, 9, 3143.	2.4	0
35	3D PET/CT 82Rb PET myocardial blood flow quantification: comparison of half-dose and full-dose protocols. European Journal of Nuclear Medicine and Molecular Imaging, 2020, 47, 3084-3093.	6.4	10
36	Transient ischaemic dilation and post-stress wall motion abnormality increase risk in patients with less than moderate ischaemia: analysis of the REFINE SPECT registry. European Heart Journal Cardiovascular Imaging, 2020, 21, 567-575.	1.2	21

Υυκά Οτακι

#	Article	IF	CITATIONS
37	Standardized volumetric plaque quantification and characterization from coronary CT angiography: a head-to-head comparison with invasive intravascular ultrasound. European Radiology, 2019, 29, 6129-6139.	4.5	50
38	Decrease in LDL-C is associated with decrease in all components of noncalcified plaque on coronary CTA. Atherosclerosis, 2019, 285, 128-134.	0.8	6
39	Effect of tube potential and luminal contrast attenuation on atherosclerotic plaque attenuation by coronary CT angiography: In vivo comparison with intravascular ultrasound. Journal of Cardiovascular Computed Tomography, 2019, 13, 219-225.	1.3	14
40	Relationship between changes in pericoronary adipose tissue attenuation and coronary plaque burden quantified from coronary computed tomography angiography. European Heart Journal Cardiovascular Imaging, 2019, 20, 636-643.	1.2	129
41	Peri-Coronary Adipose Tissue Density IsÂAssociated With 18F-Sodium Fluoride Coronary Uptake in Stable Patients WithÂHigh-Risk Plaques. JACC: Cardiovascular Imaging, 2019, 12, 2000-2010.	5.3	129
42	Improved Evaluation of Lipid-Rich Plaque at Coronary CT Angiography: Head-to-Head Comparison with Intravascular US. Radiology: Cardiothoracic Imaging, 2019, 1, e190069.	2.5	9
43	Deep Learning Analysis of Upright-Supine High-Efficiency SPECT Myocardial Perfusion Imaging for Prediction of Obstructive Coronary Artery Disease: A Multicenter Study. Journal of Nuclear Medicine, 2019, 60, 664-670.	5.0	113
44	Deep Learning for Prediction of Obstructive Disease From Fast Myocardial Perfusion SPECT. JACC: Cardiovascular Imaging, 2018, 11, 1654-1663.	5.3	246
45	Fully automated analysis of attenuation-corrected SPECT for the long-term prediction of acute myocardial infarction. Journal of Nuclear Cardiology, 2018, 25, 1353-1360.	2.1	17
46	Prognostic Value of Combined Clinical andÂMyocardial Perfusion Imaging Data Using Machine Learning. JACC: Cardiovascular Imaging, 2018, 11, 1000-1009.	5.3	172
47	Non-invasive fractional flow reserve in vessels without severe obstructive stenosis is associated with coronary plaque burden. Journal of Cardiovascular Computed Tomography, 2018, 12, 379-384.	1.3	17
48	Improvement in LDL is associated with decrease in non-calcified plaque volume on coronary CTA as measured by automated quantitative software. Journal of Cardiovascular Computed Tomography, 2018, 12, 385-390.	1.3	21
49	Molecular Imaging of Vulnerable Coronary Plaque: A Pathophysiologic Perspective. Journal of Nuclear Medicine, 2017, 58, 359-364.	5.0	20
50	Motion-Corrected Imaging of the Aortic Valve with ¹⁸ F-NaF PET/CT and PET/MRI: A Feasibility Study. Journal of Nuclear Medicine, 2017, 58, 1811-1814.	5.0	23
51	Quantitative plaque features from coronary computed tomography angiography to identify regional ischemia by myocardial perfusion imaging. European Heart Journal Cardiovascular Imaging, 2017, 18, 499-507.	1.2	31
52	Quantitative global plaque characteristics from coronary computed tomography angiography for the prediction of future cardiac mortality during long-term follow-up. European Heart Journal Cardiovascular Imaging, 2017, 18, 1331-1339.	1.2	90
53	Automatic Valve Plane Localization in Myocardial Perfusion SPECT/CT by Machine Learning: Anatomic and Clinical Validation. Journal of Nuclear Medicine, 2017, 58, 961-967.	5.0	56
54	Quantitation of left ventricular ejection fraction reserve from early gated regadenoson stress Tc-99m high-efficiency SPECT. Journal of Nuclear Cardiology, 2016, 23, 1251-1261.	2.1	25

Υυκά Οτακι

#	Article	IF	CITATIONS
55	SYNTAX Score Derived From Coronary CT Angiography for Prediction of Complex Percutaneous Coronary Interventions. Academic Radiology, 2016, 23, 1384-1392.	2.5	11
56	Predictors of high-risk coronary artery disease in subjects with normal SPECT myocardial perfusion imaging. Journal of Nuclear Cardiology, 2016, 23, 530-541.	2.1	39
57	Gender differences in the prevalence, severity, and composition of coronary artery disease in the young: a study of 1635 individuals undergoing coronary CT angiography from the prospective, multinational confirm registry. European Heart Journal Cardiovascular Imaging, 2015, 16, 490-499.	1.2	29
58	Coronary calcium scoring from contrast coronary CT angiography using a semiautomated standardized method. Journal of Cardiovascular Computed Tomography, 2015, 9, 446-453.	1.3	25
59	Relationship Between Quantitative Adverse Plaque Features From Coronary Computed Tomography Angiography and Downstream Impaired Myocardial Flow Reserve by ¹³ N-Ammonia Positron Emission Tomography. Circulation: Cardiovascular Imaging, 2015, 8, e003255.	2.6	55
60	Relationship of epicardial fat volume from noncontrast CT with impaired myocardial flow reserve by positron emission tomography. Journal of Cardiovascular Computed Tomography, 2015, 9, 303-309.	1.3	23
61	Optimizing Image Contrast Display Improves Quantitative Stenosis Measurement in Heavily Calcified Coronary Arterial Segments on Coronary CT Angiography. Academic Radiology, 2014, 21, 797-804.	2.5	8
62	Incremental Value of Diagonal Earlobe Crease to the Diamond-Forrester Classification in Estimating the Probability of Significant Coronary Artery Disease Determined by Computed Tomographic Angiography. American Journal of Cardiology, 2014, 114, 1670-1675.	1.6	8
63	Interscan reproducibility of quantitative coronary plaque volume and composition from CT coronary angiography using an automated method. European Radiology, 2014, 24, 2300-2308.	4.5	49
64	Prognostic utility of coronary computed tomographic angiography. Indian Heart Journal, 2013, 65, 300-310.	0.5	6
65	Impact of Family History of Coronary Artery Disease in Young Individuals (from the CONFIRM Registry). American Journal of Cardiology, 2013, 111, 1081-1086.	1.6	58
66	What have we learned from CONFIRM? Prognostic implications from a prospective multicenter international observational cohort study of consecutive patients undergoing coronary computed tomographic angiography. Journal of Nuclear Cardiology, 2012, 19, 787-795.	2.1	35
67	Relation of Diagonal Ear Lobe Crease to the Presence, Extent, and Severity of Coronary Artery Disease Determined by Coronary Computed Tomography Angiography. American Journal of Cardiology, 2012, 109, 1283-1287.	1.6	67
68	The relationship between epicardial fat volume and incident coronary artery calcium. Journal of Cardiovascular Computed Tomography, 2011, 5, 310-316.	1.3	26
69	Increase in epicardial fat volume is associated with greater coronary artery calcification progression in subjects at intermediate risk by coronary calcium score: A serial study using non-contrast cardiac CT. Atherosclerosis, 2011, 218, 363-368.	0.8	97
70	Threshold for the Upper Normal Limit of Indexed Epicardial Fat Volume: Derivation in a Healthy Population and Validation in an Outcome-Based Study. American Journal of Cardiology, 2011, 108, 1680-1685.	1.6	58